

Experimental and Simulation-Based Estimation of Interface Power During Physical Human-Robot Interaction in Hand Exoskeletons

Saad N. Yousaf¹, Gaurav Mukherjee¹, Raymond King¹, and Ashish D. Deshpande¹

Abstract—Even the best wearable robots face challenges with power losses in the system, especially at the physical attachment interface. While some sources for power loss are inherent to the system, such as human soft tissue or musculoskeletal joint damping, other sources such as soft padding materials and bias strap forces can be modulated to optimize interface power transmission. Few methods currently exist for estimating power loss at physical human-robot interfaces, especially for upper-body exoskeletons. This letter presents a novel method to estimate interface power from experimental data in a wearable hand device, along with a simulation model for predicting interaction behavior by incorporating viscoelastic properties at the attachment interface. The experimental method is implemented with the Maestro hand exoskeleton, and repeatability of the interface power estimation is confirmed with pilot human testing. Simulation results are compared with experimental estimation of interface power, showing agreement of trends and validating the use of a simulation model to predict physical human-robot interaction behavior. These findings highlight the advantages of multi-body simulations as a tool to perform modular, inexpensive, and predictive investigations in physical human-robot interaction, without affecting the real-world mechatronic system or hindering the subject's safety. The proposed tools for experimental estimation of interface power and simulation modeling can optimize the design and control of robots for seamless integration with the human body.

Index Terms—Physical human-robot interaction, design and human factors, wearable robotics, human-centered robotics.

I. INTRODUCTION

WEARABLE robotic devices are being developed and studied for a variety of applications including rehabilitation, assistance, human augmentation, and haptics [1], [2], [3], [4]. A fundamental principle driving the function of wearable robots is controlled power transmission between the human and the device, the nature of which can depend on the desired application. Much research has gone into maximizing the mechanical

Manuscript received 15 March 2023; accepted 24 August 2023. Date of publication 23 October 2023; date of current version 2 February 2024. This letter was recommended for publication by Associate Editor K. Mombaur and Editor A. Bera upon evaluation of the reviewers' comments. This work was supported in part by National Science Foundation (NSF) Graduate Research Fellowship Program (GRFP) and in part by Meta Reality Labs. (Corresponding author: Ashish D. Deshpande.)

Saad N. Yousaf and Ashish D. Deshpande are with the Department of Mechanical Engineering, The University of Texas, Austin, TX 78712 USA (e-mail: yousaf@utexas.edu; ashish@austin.utexas.edu).

Gaurav Mukherjee and Raymond King are with Meta Reality Labs Research, Redmond, WA 98052 USA (e-mail: gauravatoculus@meta.com; raymond.king.robot@gmail.com).

Digital Object Identifier 10.1109/LRA.2023.3326679

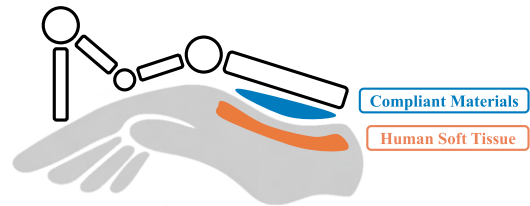


Fig. 1. Mechanical power from wearable devices is transmitted to the human user through physical human-robot interfaces, where compliance from biological tissue and soft attachment materials can lead to unintended interface power.

power that wearable devices can provide [5] while refining control strategies for physical human-robot interaction (pHRI) [6]. However, unintended losses in power transmission can lead to ineffective implementation of wearable devices, specifically due to losses at the physical human-robot interface. There are limited recent works that have studied this issue [7], and a primary challenge is the lack of easily implementable methods for reliable measurement of interface power during interaction.

Unintended losses to interface power stem from the viscoelastic compliance of biological soft tissue and soft materials at the physical attachment (Fig. 1). The physical human-robot interface (also referred to as pHRI interface, attachment interface, or physical interface) is based on the various design mechanisms used to physically attach wearable robots to the user, including cuffs, straps, handles, and others. These attachment points are the avenue for mechanical power transfer between the robot and the human, but many confounding factors make interface power transmission far from ideal. The viscoelastic properties of biological soft tissue allow for the storage and dissipation of energy during pHRI [8], [9], further confounded by changing dynamics due to muscle activation [10]. There are additional compliant elements on the robot interface such as foam padding and flexible straps, especially in the case of soft exosuits [11], [12], [13]. During wearable device use, all of these factors affect force application, leading to deformation and displacement that causes power transmission loss into the physical interface.

While ongoing research targets improvements in pHRI interfaces, the focus currently is on kinematic misalignment and interaction forces, and interface power has been overlooked. Kinematic misalignment is commonly used to evaluate errors caused from relative human-robot motion [14], [15], which not only causes errors in human joint position estimation but leads to unsafe user conditions [16]. Interaction forces are also

used to assess pHRI, either at concentrated points with load cells or throughout a surface with distributed sensorization [17], [18]. While these metrics provide valuable insight in relation to kinematic errors and improving user ergonomics, they fail to directly measure interface power, limiting our understanding of how the intended transmission of mechanical power is hindered before it reaches the human. In reality, a portion of mechanical power is stored and dissipated at the interface, which is important for wearable device design and effective interaction control in human-robot systems. Previous approaches for measuring interface power in lower-body devices [7] require costly instrumentation such as motion capture and end-effector force measurement, and this method has not been expanded to upper-body devices, especially at the human hand where there are additional challenges such as kinematic complexity and limited workspace.

In addition to establishing interface power as a functional metric for evaluating pHRI, there is a need for simulation models to study physical human-robot interaction at attachment interfaces. While real-world experiments require advanced instrumentation, time-intensive testing, and user safety, simulation-based approaches are not limited by these constraints, enabling pHRI analysis through easier measurement of desired performance metrics without hindering user safety. The cost-effective and rapid exploration of the design and control space through simulation informs the expected trends during physical human-robot interaction, making pHRI simulation a strong tool for wearable robotics research. Previous works have proposed pHRI simulation models [9], [11] which include viscoelastic properties at physical interfaces within the kinematics of the human-robot system. Although previous models have measured established pHRI performance metrics such as kinematic misalignment [14] or distributed interaction loads [17], they are also well-suited to analyzing interface power without being restricted by the sensing limitations of a real-world human-robot system.

In this work, we present i) a novel method to experimentally estimate interface power in a wearable device and ii) a simulation model to predict interface power during pHRI. The Maestro hand exoskeleton (Fig. 2) is used to implement the interface power estimation method to showcase its reliability, and experimental results are compared with pHRI simulation model output.

II. METHODS

The method for interface power estimation is formulated for a general case. The Maestro hand exoskeleton testbed is used to implement the measurement of interface power in a wearable hand device, and experiments are performed to confirm repeatability and observe trends in response to different actuation inputs. A pHRI simulation model is developed to predict interface power and energy loss, and measurements from simulation analysis are compared with results from Maestro experimentation.

A. Interface Power Calculation

The application of power to impart interaction forces is a foundational working principle for wearable robotic devices, and a representation of the overall power flow is shown in (1).

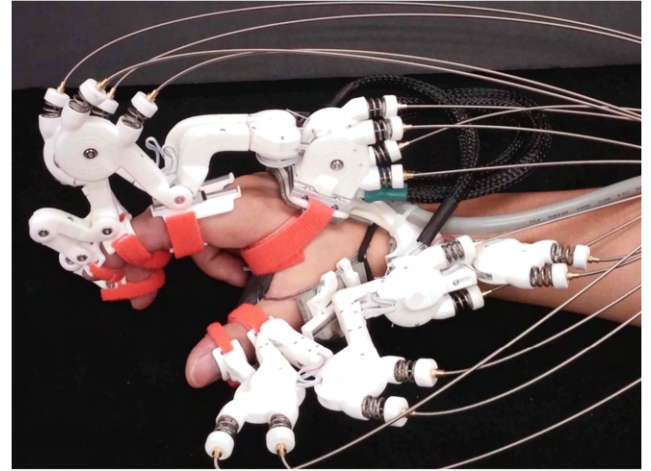


Fig. 2. Maestro hand exoskeleton has three digit modules (index finger, middle finger, and thumb), measuring position and torque across eight actuated degrees of freedom.

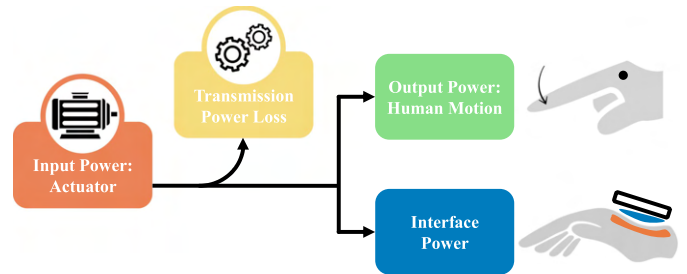


Fig. 3. Power flow diagram shows that after accounting for losses to actuator transmission, input power is divided between human motion output and interface power.

The power applied into the human-robot system from the device originates from actuators. This power then drives human motion, which is the intended purpose, but some power is also dissipated to the pHRI attachment interfaces and to frictional losses, both of which are unintended.

$$P_{in,actuator} = P_{out,human} + P_{interface} + P_{friction} \quad (1)$$

$$E_{interface} = \int_{t_1}^{t_2} P_{interface} dt \quad (2)$$

In this study, the estimation of interface power ($P_{interface}$) is accomplished by defining the other terms on the right side of (1) and isolating the desired interface power measurement. The human hand is grounded in this framework, allowing the power output to human joint motion ($P_{out,human}$) to be assumed as zero. In addition, the main source of frictional losses in our experiment setup is accounted for by modeling losses in the Bowden cable actuation, which results in a backlash hysteresis between the input motor and the output robot joint. The resulting estimation for interface power can be studied as time-series data and also as the energy change over a given time window (2). This corresponds to a measure of

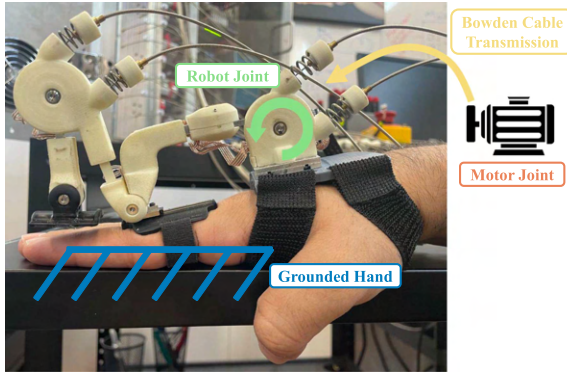


Fig. 4. In the experiment setup, the hand is grounded to eliminate any robot power being used for human joint motion. The subject is instructed to keep their palm grounded against a flat surface while staying relaxed to minimize muscle activation. The robot MCP joint is actuated through a Bowden cable SEA, and the measured angle and torque are used to calculate interface power.

work absorbed from or returned to the human-robot attachment interface.

B. Maestro Hand Exoskeleton

The Maestro hand exoskeleton (Fig. 2) has been designed for a variety of applications such as rehabilitation, assistance, and haptics [19], [20]. It is ideally suited as a research testbed with advanced sensing and actuation throughout its eight degrees of freedom (DOFs) across three digits. The primary interface of the Maestro exoskeleton is a dorsal plate that is attached to the back of the hand. Smaller attachment interfaces are also used on the finger phalanges. In this study, only the MCP joint of the index finger is used with a dorsal plate that has two velcro straps for attachment (Fig. 4).

$$P_{joint} = \tau_{joint} \dot{\theta}_{joint} = P_{out, human} + P_{interface} \quad (3)$$

The instrumentation on Maestro measures robot joint angle and robot joint torque. After differentiation of joint angle, the product of joint velocity and joint torque are used to calculate instantaneous power across the robot joint (3). Since we include a Bowden cable backlash model to measure robot joint torque, the term (P_{joint}) has already accounted for transmission losses between the actuator and the robot joint. In the proposed approach, the elimination of human motion results in the calculated power across the exoskeleton joint being a measure for interface power.

1) *Bowden Cable Series Elastic Actuation*: Series elastic actuators (SEAs) based on a Bowden cable mechanism are used in the Maestro hand exoskeleton (Fig. 5). The main source of power loss through actuation in Maestro comes from backlash in the Bowden cables. Yun et al. presented a forward backlash model (4) for accurate torque measurement and an inverse backlash model for improved torque control [21]. We implement the previously proposed forward backlash model and introduce optimization during the calibration step to eliminate the need for selecting model parameters by hand.

$$\tilde{\theta}_j(t) = BL(\theta_m(t)) \quad (4)$$

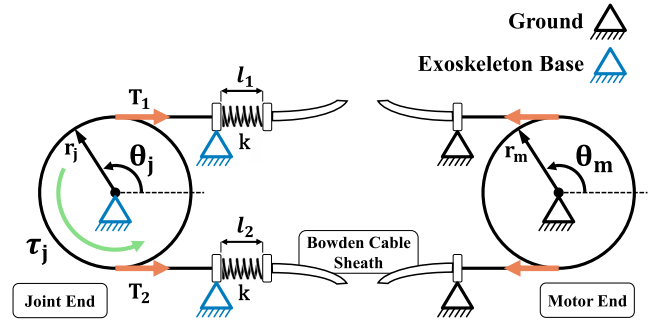


Fig. 5. Bowden cable series elastic actuators (SEAs) are driven from the motor pulley to the joint pulley. The linear displacement of springs is used to measure robot joint torque.

$$\begin{cases} \alpha(\theta_m(t) - c_r), & \dot{\theta}_m > 0; \theta_j(t^-) = \alpha(\theta_m(t^-) - c_r) \\ \alpha(\theta_m(t) - c_l), & \dot{\theta}_m < 0; \theta_j(t^-) = \alpha(\theta_m(t^-) - c_l) \end{cases}$$

In (4), the radius ratio between the motor pulley and the joint pulley is $\alpha = r_m/r_j$, and the empirically obtained parameters are c_r and c_l , the right and left offsets of the backlash curve, respectively. The backlash calibration is performed by moving the motor angle in an increasing sinusoid to capture the entire workspace of the Bowden cable SEA. Then, a constrained optimization is performed using the `fmincon()` function from MATLAB (Mathworks Inc.) to find c_r and c_l values which minimize the error in joint angle θ_j .

$$\tau_{joint} = r_j(2k\Delta d) = 2kr_j^2(\tilde{\theta}_j - \theta_j) \quad (5)$$

The calculation method for obtaining exoskeleton joint torque from the SEA mechanism is shown in (5). The SEA spring constant k and linear displacement Δd are used along with the robot joint pulley radius r_j . The backlash model from (4) is implemented when using θ_j to estimate linear spring displacement. Inclusion of the backlash model and our improvements to it result in a more accurate measurement of exoskeleton joint torque [21], leading to a more accurate measure of interface power based on (3).

C. Maestro Experiment Protocol

Pilot experiments are performed to establish the proposed method to measure interface power. After Maestro is donned, the subject's hand is grounded against a flat surface to eliminate human joint motion. The MCP joint of the Maestro hand exoskeleton is actuated in motor position control, following a sinusoidal trajectory with a prescribed amplitude and frequency. One trial is defined as five repetitions of the sine wave input, with the middle three repetitions taken for analysis.

As the exoskeleton joint is actuated in a sinusoid, the attachment interface experiences loading in two directions which correspond to two motions during regular operation: MCP flexion and MCP extension. Within each motion, the first half corresponds to loading in which power is transferred from the robot to the interface, and the second half corresponds to unloading in

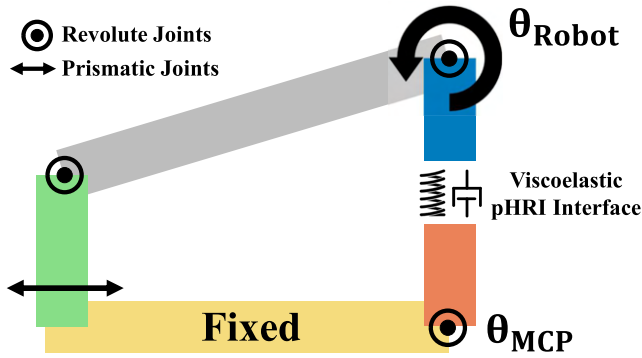


Fig. 6. Simulation model in Simscape Multibody to capture pHRI behavior in a human-robot system across the MCP joint of the hand. The viscoelastic properties included at the dorsal attachment interface determine pHRI behavior in the simulation output, which is analyzed as interface power for this study.

which power is returned from the interface to the robot. During this process, some power is lost to viscous interface elements (soft tissue, foam padding, compliant straps). Interface power measurements over time during each motion can be used to calculate the ratio of energy returned during unloading to energy absorbed during loading, which provides a measure of energy loss percentage at the interface (6). In this study, the energy loss during each flexion motion is calculated and used for analysis. The flexion motion is preferred because the accuracy of interface power estimation during the extension motion is limited due to the hand grounding method. To establish the repeatability of interface power measurement, a pilot experiment is performed with one subject in which the robot is re-donned between five consecutive trials. Confounding factors which can affect pHRI behavior are kept as consistent as possible. These include the strap tension and placement of interfaces on the subject, which are marked on the hand before the first trial and maintained throughout. The subject is also instructed to relax their hand to eliminate effects of muscle activation on interface soft tissue. The mean and standard deviation of the energy loss percentage is reported for analysis for three repetitions within each trial and also for all 15 repetitions across five trials considered together.

$$\eta_{interface} = (1 - E_{unloading}/E_{loading}) \times 100\% \quad (6)$$

In addition to repeatability testing, we also perform a pilot experiment with three human subjects to measure interface power across a range of amplitudes for the input sinusoid actuation. Five total amplitudes are tested for the commanded motor position: 6, 8, 11, 15, 20, and 25 degrees. For each amplitude, five sinusoidal oscillations are performed in succession, and we use the middle three flexion motions to calculate three energy loss measurements per trial. Between each amplitude trial, there is a 3 s resting period to allow transient effects to dissipate.

D. pHRI Simulation in Simscape Multibody

A simulation model for the physical human-robot interface has been developed in Simscape Multibody, a mechanics simulation environment within Simulink (Mathworks Inc.) (Fig. 6). Viscoelastic properties are included at the pHRI interface

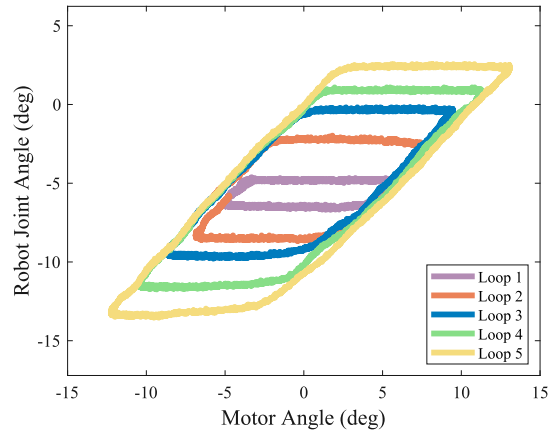


Fig. 7. Backlash calibration data from the index finger MCP joint in Maestro. As the motor is actuated through an increasing sinusoid, the robot joint follows with horizontal offsets due to Bowden cable backlash. The calibration is performed on the robot system alone without a human user.

corresponding to Maestro’s dorsal attachment based on stiffness and damping properties of human soft tissue and foam padding, as found in literature [9], [22]. The simulation input in this study is the commanded position trajectory for the robot joint. Without being restricted to real-world instrumentation, the simulation output is the power measured across the viscoelastic element, which corresponds to power measured across the dorsal attachment interface. Thus, the simulation model allows for a more direct measurement of interface power. In this study, the simulation input is a single sinusoid oscillation commanded to the robot joint position, and a range of five sinusoids amplitudes is tested in simulation, corresponding to the range of amplitudes tested through Maestro experimentation.

III. RESULTS

A. Backlash Model and Interface Power Measurement

The backlash calibration data measured from the index finger MCP joint of the Maestro hand exoskeleton is shown in Fig. 7. The time-series data for one trial is shown in Fig. 8 where motor angle and robot joint angle are measured from Maestro instrumentation. Using the established forward backlash model, the exoskeleton joint torque is calculated and used along with the differentiated exoskeleton joint angle to calculate power over time. Since the hand is grounded and the primary frictional losses in the Bowden cable actuation are accounted for in the backlash model, the calculated measure corresponds to interface power. Integration of power versus time over a specific time window results in the energy transferred during that period.

B. Repeatability of Interface Power and Energy Loss

The interface power during three repetitions of the flexion motion are shown in Fig. 9 for five separate trials. The Maestro hand exoskeleton is re-donned between each trial, and the variability across trials relates to repeatability of the interface power estimation. The mean and standard deviation for the calculated energy loss efficiency are reported in Table I, both within each trial and overall across all trials. In

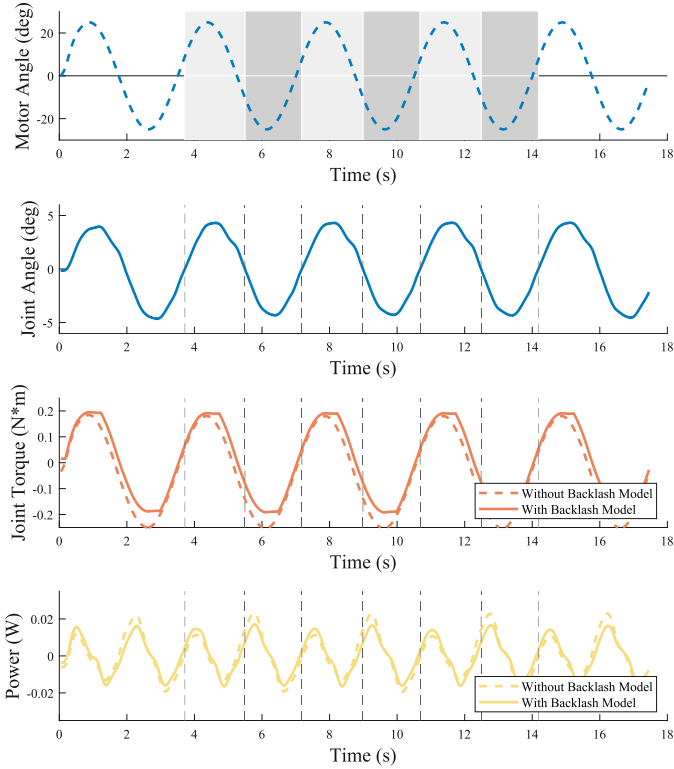


Fig. 8. Time series data from one trial with five sinusoidal repetitions of motor position. The motor angle and robot joint angle are measured from Maestro’s sensors. The joint torque is calculated through the SEA, and the resulting interface power versus time is calculated using joint torque and joint velocity. The two motions are highlighted (light grey = MCP flexion, dark grey = MCP extension).

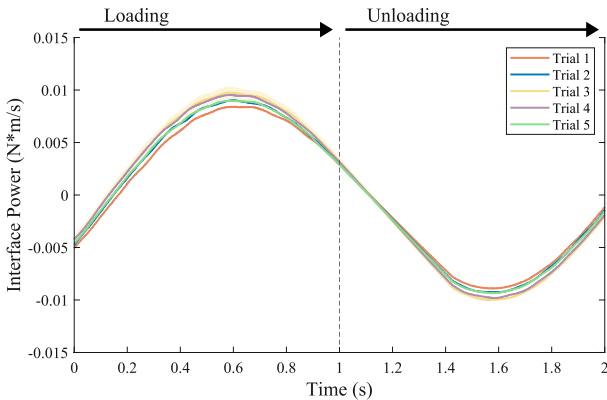


Fig. 9. Repeatability results validate the estimation method for interface power. Each line is the average of three repetitions of MCP flexion within a given trial, and the shaded area shows one standard deviation. The dotted vertical line marks the switch from interface loading to interface unloading.

TABLE I
ENERGY LOSS FOR THE REPEATABILITY STUDY

	Mean	Std. Dev.
Trial 1	48.33%	1.224%
Trial 2	42.14%	0.575%
Trial 3	48.90%	3.886%
Trial 4	46.16%	0.216%
Trial 5	46.53%	2.094%
Overall	46.41%	3.016%

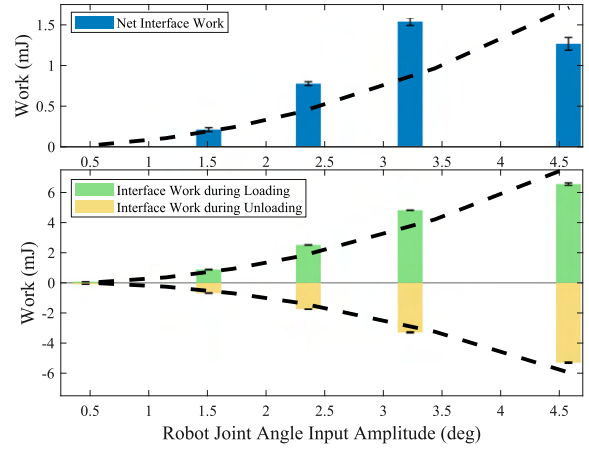


Fig. 10. Interface work for the first subject during flexion across a range of joint angle amplitudes. The bars show experimental data, and the dotted lines show simulation results. Error bars show standard error across three repetitions.

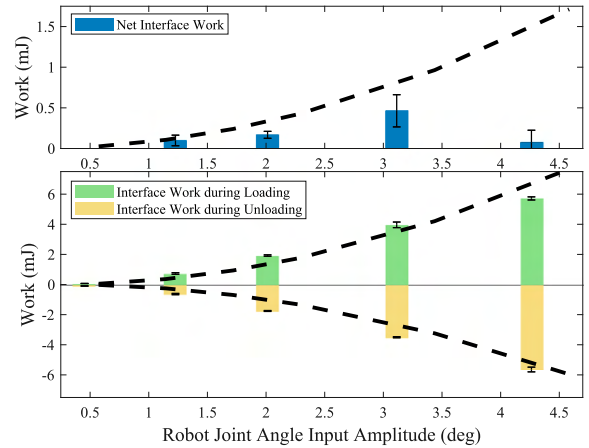


Fig. 11. Interface work for the second subject during flexion across a range of joint angle amplitudes. The bars show experimental data, and the dotted lines show simulation results. Error bars show standard error across three repetitions.

addition, the maximum root-mean-square error (RMSE) across all repeatability experiments was 0.359 milliwatts, which is 3.79% of the peak interface power.

C. Experimental Estimation of Interface Power

Interface power across Maestro’s human-robot system is estimated during experiments with three pilot subjects across a range of amplitudes for the sinusoid input robot joint position. For three flexion windows in a given trial, the interface work during loading and unloading is calculated by integrating the interface power over time. The net interface work is also calculated as the sum of work during interface loading and work during interface unloading. Results are shown for each of the pilot subjects in Figs. 10, 11, and 12.

D. Simulation Analysis of Interface Power

Interface power is directly measured in the pHRI simulation model across a range of amplitudes for the sinusoid input robot

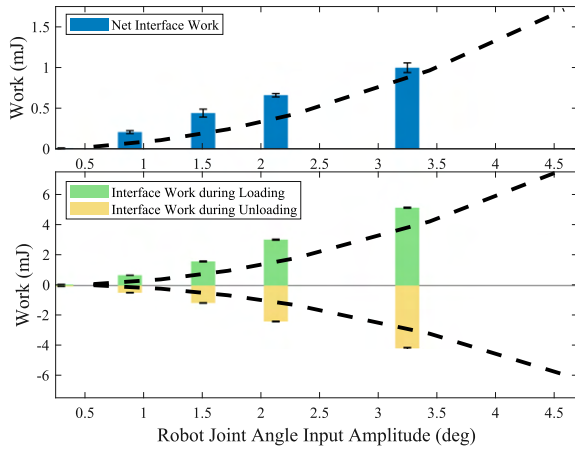


Fig. 12. Interface work for the third subject during flexion across a range of joint angle amplitudes. The bars show experimental data, and the dotted lines show simulation results. Error bars show standard error across three repetitions.

TABLE II

INTERFACE WORK ROOT MEAN SQUARE ERROR (RMSE) FOR EXPERIMENT VERSUS SIMULATION

RMSE	Net Work RMSE	Loading Work RMSE	Unloading Work RMSE
Subject 1	0.394 mJ	0.762 mJ	0.390 mJ
Subject 2	0.670 mJ	0.570 mJ	0.600 mJ
Subject 3	0.197 mJ	1.037 mJ	0.864 mJ
Overall	0.259 mJ	0.812 mJ	0.647 mJ

TABLE III

INTERFACE WORK ROOT MEAN SQUARE ERROR (RMSE) NORMALIZED FOR EXPERIMENT VERSUS SIMULATION

Normalized RMSE	Net Work RMSE	Loading Work RMSE	Unloading Work RMSE
Subject 1	23.4%	10.0%	6.59%
Subject 2	45.7%	8.67%	11.74%
Subject 3	23.1%	27.8%	30.0%
Overall	27.3%	10.7%	10.9%

joint position. During flexion, the interface work from loading and unloading, as well as the net interface work, is calculated by integrating the interface power over time. The simulation results are plotted over the experimental results in Figs. 10, 11, and 12 to provide a direct comparison. Furthermore, Table II shows the RMSE values for interface work when experimental results are compared to simulation, and Table III shows the same RMSE values normalized to the range of the predicted interface work in simulation.

IV. DISCUSSION

This letter presents a method for the estimation of interface power during physical human-robot interaction. Validation through experiments and simulation using a wearable hand exoskeleton demonstrate the method's repeatability and importance for pHRI research. The implementation of a forward backlash model in the Bowden cable SEA with the addition of optimization to improve the calibration process accounts for the biggest source of power loss from actuation transmission

(Fig. 7). With the grounded human hand in this framework, we demonstrate the experimental estimation of interface power in wearable hand devices.

The repeatability of the presented approach is shown in Fig. 9 and Table I. Interface power measurements show strong consistency across multiple repetitions within the same trial, with slightly worse repeatability across trials. The differences across trials result from re-donning of Maestro, highlighting that confounding factors related to the pHRI attachment interface have an appreciable effect on interface power estimation. These factors can include minor differences in interface location on the hand and strap tensioning across the palm.

With the inclusion of viscoelastic properties at the pHRI interface, the simulation model predicts interaction behavior in a wearable robot system. A comparison of simulation results and experimental data shows a strong agreement of trends (Figs. 10–12). With increasing input amplitude, the net work into the interface increases in experimentation and simulation. The same is true for increasing interface work during loading and decreasing interface work during unloading. Table II shows the RMSE values when comparing experimental results to simulation, both within subjects and overall, and Table III shows the same comparison with normalized RMSE values. The higher errors for net work are due to the smaller magnitude range of this measurement, where system errors become more prominent. These results also illustrate that subject-to-subject differences at the attachment affect experimental measurement of interface power. The agreement of experiment and simulation trends validates the estimation of interface power and proves the value of the simulation model for pHRI research.

The proposed experimental method is well-suited for the hand, where anatomical complexity and limited workspace make instrumentation challenging. This method can be extended to other parts of the body where human joints can be feasibly grounded during experiments, providing researchers with a tool that serves as the first step in estimating interface power. In larger areas of the body, more sophisticated measurement methods with advanced instrumentation [7] can be applied to measure interface power, especially during non-grounded conditions when there is human motion. Compared to previous works for lower-limb wearable devices [7], the interface power measurements in this letter are three orders of magnitude lower. However, this is expected because interaction loads for hand devices [19] are also three orders of magnitude lower than interaction loads for lower-limb devices [23], and the hand also has less soft tissue as compared to other parts of the body. We expect higher interface power magnitudes if the proposed method is applied to other areas of the human.

Experimental and simulation-based estimation of interface power are valuable tools to optimize pHRI through the design and control of wearable robots. Evaluation through interface power can inform design decisions, ranging from robot kinematics and actuation to finer interface design choices such as the use of soft materials, the level of strap tension, and the device form factor in relation to the human. Estimation of interface power can also be used in the control of wearable robotic devices to predict how much input mechanical power from the robot is delivered

to the human after accounting for pHRI losses. In addition, the simulation approach can investigate physical human-robot interaction in a time-effective and cost-effective manner, without being restricted by available instrumentation or user safety concerns. The pHRI simulation model measures interface power for this study but it can also measure other pHRI performance metrics such as kinematic misalignment and interaction loads. Through a simulation-based approach, we can rapidly explore the design and control space of a human-robot system, enabling improved pHRI that can be translated to wearable devices.

The experimental estimation of interface power for research must consider that this approach makes measurements with a grounded hand. To appropriately use the results from this method, it is best to focus on the experimentally established trends instead of the exact magnitudes. To contextualize the magnitude of estimated interface power in this study, we measured the power across Maestro's MCP joint during motion with a passive human user. The interface power in this study was between 40%–50% of the exoskeleton joint power during passive motion, indicating that pHRI improvements made using trends observed from interface power estimation will result in appreciable improvements during general device use. This method can be further contextualized by considering the interaction loads applied during testing. For example, Fig. 8 shows interaction torques up to 0.2 N-m corresponding to interface power up to 20 milliwatts. This number defines the maximum interface power that would be expected during human motion with Maestro with comparable interaction loads.

V. CONCLUSION

A novel method for the estimation of interface power in wearable devices is presented in this letter, along with a pHRI simulation model which predicts physical interaction behavior in a human-robot system. The estimation of interface power is implemented on the Maestro hand exoskeleton, and experimental results are compared with simulation analysis to verify agreement of trends. Future work can apply the proposed experimental method to measure interface power in wearable devices, both for the hand and also broadly for other parts of the body. A simulation-based approach allows for the study of many pHRI metrics such as interface power, kinematic misalignment, and interaction loads, allowing researchers to define how various factors within the domains of robot kinematics, attachment design, and interaction control affect these metrics. The future of pHRI research necessitates the use of both purposeful real-world experimentation and predictive simulation modeling, each informing the other to optimize robot design and control. The tools presented in this work enable the next generation of wearable robots that naturally extend the capabilities of the human body by optimizing physical interaction between the user and the robot.

REFERENCES

[1] S. Viteckova, P. Kutilek, and M. Jirina, "Wearable lower limb robotics: A review," *Biocybernetics Biomed. Eng.*, vol. 33, no. 2, pp. 96–105, 2013.

- [2] P. Maciejasz, J. Eschweiler, K. Gerlach-Hahn, A. Jansen-Troy, and S. Leonhardt, "A survey on robotic devices for upper limb rehabilitation," *J. Neuroeng. Rehabil.*, vol. 11, no. 1, 2014, Art. no. 3.
- [3] A. M. Dollar and H. Herr, "Lower extremity exoskeletons and active orthoses: Challenges and state-of-the-art," *IEEE Trans. Robot.*, vol. 24, no. 1, pp. 144–158, Feb. 2008.
- [4] P. E. Dupont et al., "A decade retrospective of medical robotics research from 2010 to 2020," *Sci. Robot.*, vol. 6, no. 60, 2021, Art. no. eabi8017.
- [5] B. T. Quinlivan et al., "Assistance magnitude versus metabolic cost reductions for a tethered multiarticular soft exosuit," *Sci. Robot.*, vol. 2, no. 2, 2017, Art. no. eaah4416.
- [6] J. Kim et al., "Reducing the energy cost of walking with low assistance levels through optimized hip flexion assistance from a soft exosuit," *Sci. Rep.*, vol. 12, no. 1, pp. 1–13, 2022.
- [7] M. B. Yandell, B. T. Quinlivan, D. Popov, C. Walsh, and K. E. Zelik, "Physical interface dynamics alter how robotic exosuits augment human movement: Implications for optimizing wearable assistive devices," *J. Neuroengineering Rehabil.*, vol. 14, no. 1, pp. 1–11, 2017.
- [8] A. Petron, J.-F. Duval, and H. Herr, "Multi-indenter device for in vivo biomechanical tissue measurement," *IEEE Trans. Neural Syst. Rehabil. Eng.*, vol. 25, no. 5, pp. 426–435, May 2017.
- [9] R. J. Varghese, G. Mukherjee, R. King, S. Keller, and A. D. Deshpande, "Designing variable stiffness profiles to optimize the physical human robot interface of hand exoskeletons," in *Proc. IEEE 7th Int. Conf. Biomed. Robot. Biomechatron.*, 2018, pp. 1101–1108.
- [10] S. N. Yousaf, K. Ghonasgi, P. Esmatloo, and A. D. Deshpande, "Human-robot interaction: Muscle activation and angular location affect soft tissue stiffness," in *Proc. IEEE 9th Int. Conf. Biomed. Robot. Biomechatron.*, 2022, pp. 01–06.
- [11] S. N. Yousaf, P. Esmatloo, K. Ghonasgi, and A. D. Deshpande, "A method for the analysis of physical human-robot interaction," in *Proc. IEEE/ASME Int. Conf. Adv. Intell. Mechatronics*, 2021, pp. 1249–1254.
- [12] D. M. Sengeh and H. Herr, "A variable-impedance prosthetic socket for a transtibial amputee designed from magnetic resonance imaging data," *J. Prosthetics Orthotics*, vol. 25, no. 3, pp. 129–137, 2013.
- [13] M. B. Yandell, D. M. Ziemnicki, K. A. McDonald, and K. E. Zelik, "Characterizing the comfort limits of forces applied to the shoulders, thigh and shank to inform exosuit design," *PLoS One*, vol. 15, no. 2, 2020, Art. no. e0228536.
- [14] D. Zanotto, Y. Akiyama, P. Stegall, and S. K. Agrawal, "Knee joint misalignment in exoskeletons for the lower extremities: Effects on user's gait," *IEEE Trans. Robot.*, vol. 31, no. 4, pp. 978–987, Aug. 2015.
- [15] R. Mallat, M. Khalil, G. Venture, V. Bonnet, and S. Mohammed, "Human-exoskeleton joint misalignment: A systematic review," in *Proc. IEEE 5th Int. Conf. Adv. Biomed. Eng.*, 2019, pp. 1–4.
- [16] A. Schiele, "Ergonomics of exoskeletons: Objective performance metrics," in *Proc. IEEE World Haptics 3rd Joint EuroHaptics Conf. Symp. Haptic Interfaces Virtual Environ. Teleoperator Syst.*, 2009, pp. 103–108.
- [17] K. Ghonasgi, S. N. Yousaf, P. Esmatloo, and A. D. Deshpande, "A modular design for distributed measurement of human-robot interaction forces in wearable devices," *Sensors*, vol. 21, no. 4, 2021, Art. no. 1445.
- [18] J. Tamez-Duque, R. Cobian-Ugalde, A. Kilicarslan, A. Venkatakrishnan, R. Soto, and J. L. Contreras-Vidal, "Real-time strap pressure sensor system for powered exoskeletons," *Sensors*, vol. 15, no. 2, pp. 4550–4563, 2015.
- [19] P. Agarwal, J. Fox, Y. Yun, M. K. O'Malley, and A. D. Deshpande, "An index finger exoskeleton with series elastic actuation for rehabilitation: Design, control and performance characterization," *Int. J. Robot. Res.*, vol. 34, no. 14, pp. 1747–1772, 2015.
- [20] Y. Yun et al., "Maestro: An EMG-driven assistive hand exoskeleton for spinal cord injury patients," in *Proc. IEEE Int. Conf. Robot. Automat.*, 2017, pp. 2904–2910.
- [21] Y. Yun, P. Agarwal, J. Fox, K. E. Madden, and A. D. Deshpande, "Accurate torque control of finger joints with ut hand exoskeleton through Bowden cable SEA," in *Proc. IEEE/RJS Int. Conf. Intell. Robots Syst.*, 2016, pp. 390–397.
- [22] R. J. Varghese, G. Mukherjee, and A. Deshpande, "Designing physical human-robot interaction interfaces: A scalable method for simulation based design," *Front. Neurorobot.*, vol. 15, 2022, Art. no. 727534.
- [23] F. A. Panizzolo et al., "A biologically-inspired multi-joint soft exosuit that can reduce the energy cost of loaded walking," *J. Neuroengineering Rehabil.*, vol. 13, no. 1, pp. 1–14, 2016.